

## Structural Determination in Metallic Glasses from Correlations in 4D STEM Datasets

Carter Francis, Debaditya Chatterjee, Sachin Muley and Paul Voyles

University of Wisconsin-Madison, Madison, Wisconsin, United States

4D STEM measurements,  $I(\mathbf{r}, \mathbf{k})$ , with nanometer size electron probe beams offer a unique window into the structure of glassy materials. The acquired 4D dataset can be analyzed to determine spatial fluctuations in the diffracted intensity, which is fluctuation electron microscopy (FEM) [1], or analyzed to determine the angular correlations within each pattern, which measures the rotational symmetries of the diffracting structures. Both methods provide statistical descriptions of the glass structure, and angular correlations allow for real space structure mapping [2]. Together, these methods provide complementary probes of glass structure.

FEM studies the normalized variance,  $V$ , of a 4D STEM dataset acquired with the distance between probe positions larger than the probe diameter. If we consider the diffracted intensity in polar coordinates  $\mathbf{k} = (k, \theta)$ ,

$$V(k) = \frac{\langle\langle I(\theta, k, \mathbf{r}) \rangle_{\theta}^2 \rangle_{\mathbf{r}} - \langle\langle I(\theta, k, \mathbf{r}) \rangle_{\theta} \rangle_{\mathbf{r}}^2}{\langle\langle I(\theta, k, \mathbf{r}) \rangle_{\theta} \rangle_{\mathbf{r}}^2}.$$

Angular correlations can be described by the autocorrelation function in the polar angle,  $C(k, \phi, \mathbf{r})$ , given by,

$$C(k, \phi, \mathbf{r}) = \frac{\langle I(\theta + \phi, k, \mathbf{r}) * I(\theta, k, \mathbf{r}) \rangle_{\theta} - \langle I(\theta, k, \mathbf{r}) \rangle_{\theta}^2}{\langle I(\theta, k, \mathbf{r}) \rangle_{\theta}^2}.$$

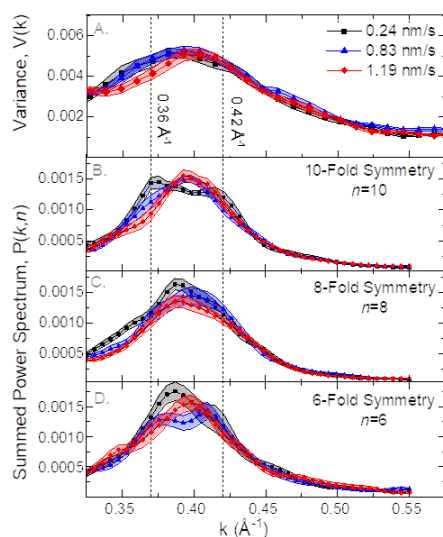
The power spectrum  $P(k, n, \mathbf{r})$  of  $C(k, \phi, \mathbf{r})$  is perhaps more useful than  $C(k, \phi, \mathbf{r})$ . Since the data are periodic in  $\theta$ , the power spectrum is a discrete representation in terms of the order of the rotational symmetry,  $n$ .  $P(k, n, \mathbf{r})$  provides a concise measure of the rotational symmetries present in a nanodiffraction pattern, and  $P(k, n)$ , which is the power spectrum of the sum of  $C$  for all  $\mathbf{r}$  in the dataset  $C(k, \phi, \mathbf{r})$ , provides a simplified and more statistically significant representation for comparison with FEM results.

Im *et al.* recently showed that samples for angular correlation analysis must be thin (on order 20 nm) or chance correlations will create unphysical odd- $n$  symmetries [2]. All the samples here were 20 nm thick or less to avoid this problem. Angular correlation analysis also requires careful correction of residual aberrations in the nanodiffraction patterns. In our data, elliptical distortion in the patterns was mitigated by fitting an ellipse to the amorphous ring created by summing all the nanodiffraction patterns over positions. Without this correction, the 2-fold correlation,  $P(k, 2)$ , is very strong, and all of the other even  $n$  correlations are significantly reduced in power.

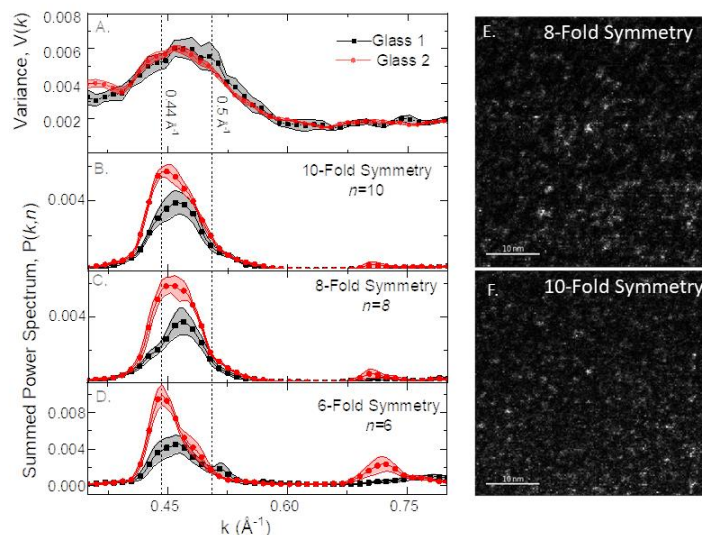
Figure 1 shows FEM and summed angular power spectrum data for a series of  $Zr_{65}Cu_{27.5}Al_{7.5}$  metallic glass thin films as a function of their deposition rate. Lower deposition rate leads to a more thermally stable glass with higher modulus and hardness. Figure 1a shows the FEM results, and Figure 1b-d shows  $P(k, n)$  for  $n = 10, 8,$  and  $6,$  respectively. The largest deviation in  $V$  for the various samples is around the peak at  $0.36 \text{ \AA}^{-1}$ , and there is an aligned peak in the 10-fold symmetry  $P(k, 10)$ . 10-fold symmetry is a signature of icosahedral structural order with crystallographically-disallowed 5-fold rotational symmetry in real space. At higher  $k$ , around  $0.42 \text{ \AA}^{-1}$ , there is an additional peak in the 6-fold symmetry  $P(k, 6)$ , suggesting that the variance feature here arises from structures with crystallographically-allowed rotational symmetry. These peak assignments provide independent confirmation of structure types discovered previously in hybrid reverse Monte Carlo simulations based on only FEM data [3].

Figure 2(a)-(d) shows FEM and spatially-averaged  $P(k, n)$  measurements from two  $Pd_{42.5}Ni_{42.5}P_{15}$  glasses, one before and one after a thermally-induced structural reordering [4]. The FEM results show a small increase in  $V$  near  $k = 0.44 \text{ \AA}^{-1}$  and a small decrease near  $0.5 \text{ \AA}^{-1}$  after annealing. The corresponding changes in  $P(k, n)$  are much larger. For  $n = 6, 8,$  and  $10,$   $P(k)$  at  $0.44 \text{ \AA}^{-1}$  is significantly higher after annealing, and  $P$  increases over all  $k$ . The overall increase indicates significantly improved structural ordering after annealing, consistent with changes in x-ray diffraction and spectroscopy [4], and shows that the changes extend to nanometer length scales.

The high speed of modern direct electron detectors makes it possible to acquire dense sampled  $I(\mathbf{k}, \mathbf{r})$  data with minimal drift. Figure 2(e) and (f) show  $P(k, n, \mathbf{r})$  for  $n = 8$  and  $10$  respectively, averaged from  $k = 0.4$  to  $0.55 \text{ \AA}^{-1}$ , but fully resolved in  $\mathbf{r}$ . The results are real space structural maps of regions with high rotational symmetry. The maps show clusters in 1-2 nm in diameter, similar to previously reported ordering length scales [2]. Determining the true size and number density of ordered clusters from these data should be possible, but requires careful consideration of the diffraction geometry of randomly oriented small clusters and the influence of the electron probe size [5].



**Figure 1.** 4D STEM structure data for a series of  $\text{Zr}_{65}\text{Cu}_{27.5}\text{Al}_{7.5}$  deposited thin films. (A) FEM showing differences in  $V(k)$  at  $k = 0.36 \text{ \AA}^{-1}$  and  $0.42 \text{ \AA}^{-1}$  for different deposition rates. (B) Summed power spectrum for  $P(k, n=10)$ , with peaks around  $k = 0.36 \text{ \AA}^{-1}$  for the slower deposited glasses (C) Summed power spectrum for  $P(k, n=8)$  (D) Summed power spectrum for  $P(k, n=6)$ , with peaks at  $k = 0.42 \text{ \AA}^{-1}$  for the faster deposition rate sample.



**Figure 2.** 4D STEM structure data for a set of  $\text{Pd}_{42.5}\text{Ni}_{42.5}\text{P}_{15}$  glasses before and after annealing. (A) FEM showing small deviations in  $V(k)$  at  $k = 0.44 \text{ \AA}^{-1}$  and  $0.53 \text{ \AA}^{-1}$  (B-D) Summed power spectrum for  $P(k, n)$  for  $n = 10, 8,$  and  $6,$  respectively. These spectra all show large increases in the power spectrum after annealing due to ordering in the glass. (E,F) Spatial maps of high rotational symmetry clusters, for  $n = 8$  and  $10,$  respectively.

## References

- [1] P.M. Voyles, D.A. Muller. *Ultramicroscopy*, 93 (2002) p. 147.
- [2] Im, S, et al. *Ultramicroscopy* 195 (2018) p. 189.
- [3] Hwang, J., et al. *Physical Review Letters*, 108(19) (2012) p. 195505.
- [4] Du, Q. et al., *Materials Today*, xxx(xx). (2019). <https://doi.org/10.1016/j.mattod.2019.09.002>
- [5] Support for this research is provided by the National Science Foundation (DMR-1807241).